energies

MDPI

Review

Current Trends for State-of-Charge (SoC) Estimation in Lithium-Ion Battery Electric Vehicles

Ingvild B. Espedal [1], Asanthi Jinasena [1], Odne S. Burheim [1] and Jacob J. Lamb [1,2,*]

[1] Department of Energy and Process Engineering & ENERSENSE, NTNU, 7491 Trondheim, Norway; ingvibes@stud.ntnu.no (I.B.E.); asanthi.jinasena@ntnu.no (A.J.); odne.s.burheim@ntnu.no (O.S.B.)
[2] Department of Electronic Systems & ENERSENSE, NTNU, 7491 Trondheim, Norway
* Correspondence: jacob.j.lamb@ntnu.no

Abstract: Energy storage systems (ESSs) are critically important for the future of electric vehicles. Despite this, the safety and management of ESSs require improvement. Battery management systems (BMSs) are vital components in ESS systems for Lithium-ion batteries (LIBs). One parameter that is included in the BMS is the state-of-charge (SoC) of the battery. SoC has become an active research area in recent years for battery electric vehicle (BEV) LIBs, yet there are some challenges: the LIB configuration is nonlinear, making it hard to model correctly; it is difficult to assess internal environments of a LIB (and this can be different in laboratory conditions compared to real-world conditions); and these discrepancies can lead to raising the instability of the LIB. Therefore, further advancement is required in order to have higher accuracy in SoC estimation in BEV LIBs. SoC estimation is a key BMS feature, and precise modeling and state estimation will improve stable operation. This review discusses current methods use in BEV LIB SoC modelling and estimation. The review culminates in a brief discussion of challenges in BEV LIB SoC prediction analysis.

Keywords: lithium-ion battery; state-of-charge; modelling; battery management systems

Citation: Espedal, I.B.; Jinasena, A.; Burheim, O.S.; Lamb, J.J. Current Trends for State-of-Charge (SoC) Estimation in Lithium-Ion Battery Electric Vehicles. *Energies* **2021**, *14*, 3284. https://doi.org/10.3390/en14113284

Academic Editor: Woojin Choi

Received: 14 April 2021
Accepted: 1 June 2021
Published: 4 June 2021

1. Introduction

Energy storage systems (ESSs) are important technologies for future electric cars and smart grids [1–4]. Lithium-ion batteries (LIBs) are the fastest growing ESS technology [5]. Despite this, the safety and management of LIBs are vital areas that still require further development [6]. Therefore, LIB management systems (BMSs) are critical for the electrification of battery electric vehicles (BEVs) and encompass a variety of features to ensure optimal operation (Figure 1).

The developing advanced and smart state-of-charge (SoC) estimators for LIBs have become an active research topic in recent years. The key technological challenges limiting the advancement of SoC can be gathered into three aspects. The first is that the LIB structure is nonlinear, making it challenging to model accurately. This is due to the multi-scale nature (e.g., active materials, cells, and battery packs are all in different spatial scales), and time scale aspects (e.g., aging). Second, the internal environment is difficult to determine and is susceptible to fluctuations of the external environment. Scaling up LIBs from laboratory- to industrial-level production decreases the correlation between calculated values and actual values, rendering it difficult to reliably determine the battery's internal states. Finally, the LIBs discrepancies directly affect the performance of the LIB pack, raising the instability of the LIB. Estimation measures designed for smaller LIBs are redundant on large-scale LIBs (i.e., BEV LIBs), and reliable and precise LIB SoC estimation is difficult. Therefore, advanced SoC methods are urgently required to overcome these challenges [7,8].

Battery state estimation is a key advanced BMS feature in BEVs. Precise modeling and state estimation will allow stable operation, facilitate optimal battery operation, and provide the fundamentals for security supervision [9]. This review discusses BEV LIB

SoC modelling, estimation and methods. The review culminates in a brief discussion of challenges in BEV LIB SoC prediction analysis.

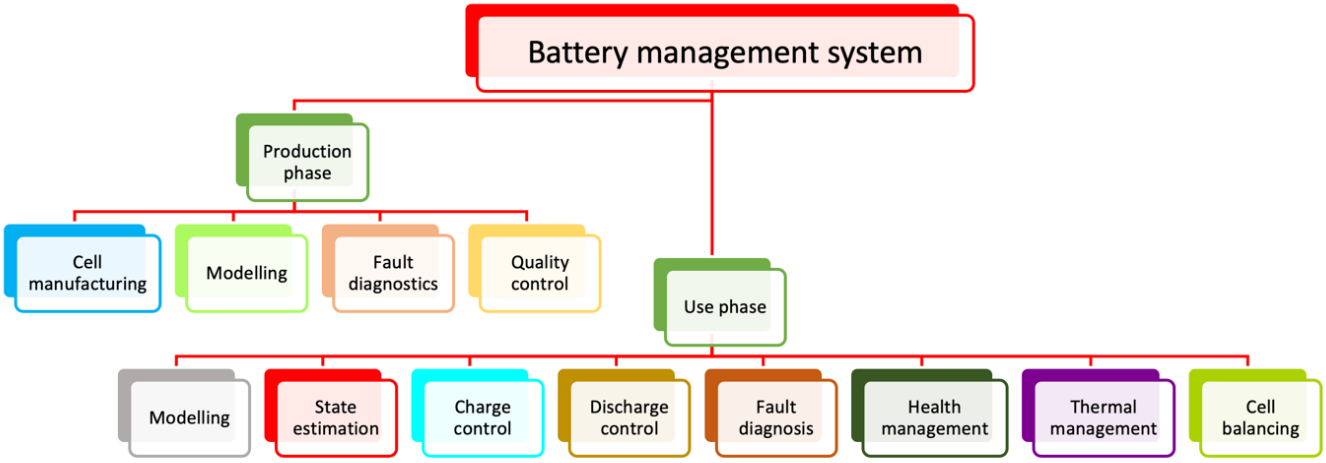

Figure 1. Battery management system (BMS) functional features for battery electric vehicle lithium-ion batteries.

2. Overview of BEV LIB SoC Modelling Approaches

The battery models are useful in model-based SoC estimation and can be characterized as physical electrochemical models [10,11], electrical equivalent circuit models [12,13] and data-driven models [14,15], with the two latter being routinely used in BEV SoC estimation. This section introduces these models with emphasis on data-driven models and electrical equivalent circuit models, and more information about their application and comparisons between the models is given in Section 4.

2.1. Physical Electrochemical Models

Single-particle models are the simplest established model for physics-based electrochemical analysis [16]. Here, a single particle reflects the Li-ion concentration distribution in the electrode. It can be used to analyze primary output and electrode solid-phase diffusion effect; however, the precision is poor. To improve the precision, a model has been developed that considers the electrolyte's effect on the output potential, suggesting a partial differential equation to conserve the liquid electrolyte material [17].

A pseudo-two-dimensional model has been developed that considers that the cell anode and cathode as porous consisting of ball-like particles with the electrolyte filling the gaps in-between [18]. As the pseudo-two-dimensional model includes multiple coupled partial differential equations, it must be condensed from the engineering perspective [19,20].

A key intention why physics-based models are hard to implement is that a huge amount of unspecified variables are required to be defined using approaches such as global optimization. Unsurprisingly, they can face overfitting or local optimization issues. Without correct and comprehensive parameters, the open loop simulations of electrochemical models based on physics are not optimal for SoC calculations. High-resolution detailed models usually contain numerous nonlinear partial differential equations, which make the model solving complex and computationally expensive, and is not suitable for estimation online, despite the high accuracy. There are reduced-order models that are less complex and take less computational time than the full-order models and can be used in online estimation applications [21]. However, these advantages come with the cost of increased estimation errors.

2.2. Electrical Equivalent Circuit Models

Electrical equivalent circuit models have grown in popularity due to their simpler construction, allowing implementation into real-time applications. Models of electronic

counterparts use electrical components to imitate LIB behavior. These can be classified into integral-order and fractional-order models.

2.2.1. Integral-Order Models

Most of the commonly used equivalent circuit models are integral-order models. Of these, the R_{int} model is the most used integral-order model [22]. The R_{int} model structure is straightforward; however, it does not consider the polarization and diffusion dynamics. Liaw et al. [23] introduced the resistor–capacitor model, which is a first-order model capable of mimicking LIB charging and discharging behavior using one resistor–capacitor network. Additionally, the open-circuit voltage hysteresis behavior can be considered to improve model accuracy [24].

The LIBs input/output relationship is simple to infer for integral-order analogous circuit models. Therefore, the most frequently used technique for online parameter detection is the least-squares recursive algorithm. A co-estimator has also been recommended to predict model parameters and battery status [25]. This can be in the form of identification of parameters while considering the electrochemical properties [26], or a multi-objective genetic algorithm [27].

2.2.2. Fractional-Order Models

Fractional-order calculus-based models are also common in modeling due to their fractional characteristics. Electrochemical impedance spectroscopy (EIS) is an accurate method for modeling electrochemical reactions of lithium ions. However, it is quite difficult to estimate SoC using only EIS; therefore, many fractional-order models are used together with EIS for a better estimation [28]. There are some studies that use Bode plots [29] to aid the circuit models for improved estimation. However, in order to use electrical equivalent circuit models for efficient online SoC estimation, a proper parameter identification method (either online or offline) such as curve fitting, recursive least square, particle swarm, or genetic algorithm must be used.

Constant phase elements can also be utilized in resistor–capacitor networks instead of capacitors [30]. Using simplified fractional-order impedance, a genetic algorithm can be applied to classify model constraints obtaining an error of 0.5% [31]. Alternatively, non-integer model derivatives with a particle swarm optimization algorithm can be used to classify model constraints with strong accuracy and robustness [32]. Fractional-order equivalent circuit models with alternatives of Kalman filter are commonly used to estimate SoC in LIBs [33,34].

2.3. Data-Driven Models

Data-driven approaches are commonly used to design LIB models. Most used data-driven methods for online SoC estimation are based on machine learning techniques (e.g., neural networks, support vector machines, and fuzzy logics). LIB testing experiments have confirmed the successful solution proposed using a neural-based thermal-electric-coupled model [35]. It is also possible to perform data estimation by integrating the neural network with particle filtering [36]. Dynamic simulation technology is commonly used in LIB modelling, and a recent Monte Carlo 3D model has been used to show the structural evolution of solid sulfur and lithium sulfide dissolution/precipitation during lithium-sulfur battery discharge [37]. The kinetic model can estimate battery subtleties over longer scales of time. While data-driven techniques work well on nonlinear issues, they can be affected by the datasets and methods used for training. Further, the requirement of large data set to cover all the possible operating conditions, demand high overall computational costs.

3. State Estimation in BEV LIBs

A BEV LIB is a dynamic, nonlinear device of several state variables, so correct state prediction is the secret to controlling and the foundation for LIB power. This section

defines SoC and parameters routinely used in BEVs for SoC estimation and summarizes the commonly used LIB state estimation methods.

3.1. SoC in LIBs

SoC is the measure of the remaining energy in a battery (Figure 2). Physically, the amount of energy left in a battery (ψ) is defined as the average concentration of lithium-ions in the cathode ($C_{s,avg}$) over the maximum possible concentration:

$$\psi = \frac{C_{s,avg}}{C_{s,max}} \tag{1}$$

Theoretically, $\psi = 0$ and $\psi = 100$ is possible; however, it is not feasible as the removal of too many lithium-ions from the cathode will damage the structure and increase degradation. Therefore, a ψ window is defined for LiBs where $\psi_{0\%} > 0$ and $\psi_{100\%} < 1$. The SoC can now be defined by a ratio of the defined ψ windows:

$$\text{SoC} = \frac{\psi_k - \psi_{0\%}}{\psi_{100\%} - \psi_{0\%}} \tag{2}$$

where ψ_k is the amount of energy left in the battery at time k. This definition of SoC is theoretically correct; however, it is not practically possible for a BMS to calculate ψ as the concentration of lithium-ions cannot be measured directly. As a consequence, a definition of SoC that is not directly based on the lithium-ion concentration is required. SoC can therefore be explained as the LIBs residual power ratio (C_r) to maximum available capacity (C_a) (Equation (3)) [38,39]. C_r is the residual energy that can be drained from the LIB over time. C_r is affected by cycling and deterioration of the LIBs electrochemical aspects. C_a is the highest possible load capacity that can be collected during the initial cycle period under diverse conditions. C_a is unable to reach the rated power (C_{rated}) (i.e., the manufacturer's LIB capacity for regular operation). The importance of a LIBs C_a relies on the state-of-health (SoH) and current discharge volume. The SoC is expressed in percentage between 100% (fully charged) and 0% (fully discharged; Figure 2).

$$\text{SoC}(t) = \left(\frac{C_r}{C_a}\right) \cdot 100\% \tag{3}$$

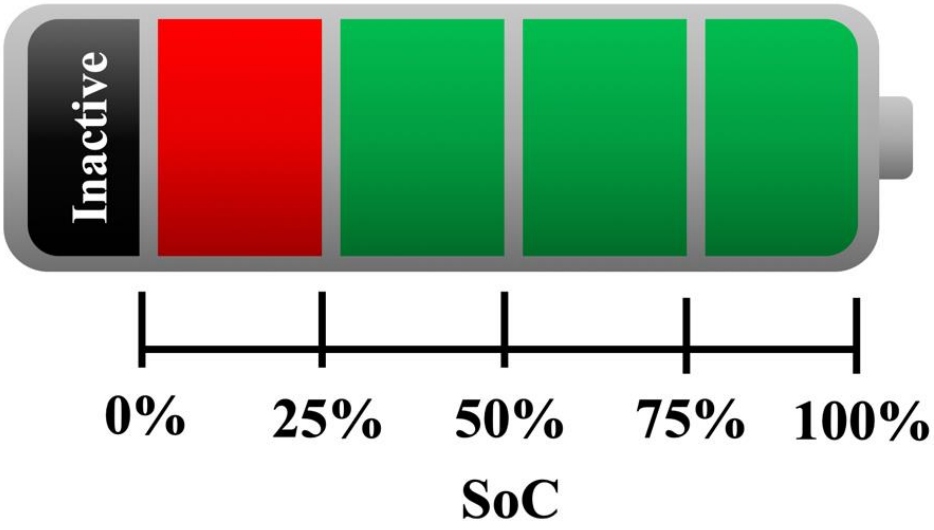

Figure 2. Stored energy status of a lithium-ion battery related to state-of-charge.

3.1.1. Coulomb Counting

Coulomb counting is a simple classical SoC estimation method. Coulomb counting is utilized to find the connection between the SoC and the cycling of the LIB. The SoC(t) can usually be determined through this method (Equation (4)), where the coulombic efficiency is denoted η_i, the initial SoC is denoted SoC(0), and the battery charging/discharging current is denoted as $I(t)$. Commonly, η_i represents the ratio between the consumed and available electrons, while cycling the LIB (a ratio of 0.9 during charging, and 1 during discharging) [40]. Despite this, the coulombic charging efficiency ranges from 0.9 to 1 with changes in the conditions of operation (e.g., the current rate and temperature) [41].

$$\mathrm{SoC}(t) = \mathrm{SoC}(0) + \int_0^t \frac{\eta_i I(t)}{C_a} \cdot \Delta t \tag{4}$$

Large errors can occur in this method due to accumulation of terminal measurements, which require frequent calibrations [42]. Despite the easy implementation, error accumulation and the initial SoC value requirement [43] make this approach not ideal for online SoC estimation.

3.1.2. Open Circuit Voltage

The open circuit voltage (OCV) is a significant value that is routinely used to characterize electrochemical cells (i.e., batteries). Despite this, there is no common description for it [44]. In general, it is described as the voltage determined by a potentiometer between the cathodic and anodic poles of the electrochemical cell when the cell has reached thermodynamic equilibrium [45]. As the status of whether the cell is in equilibrium is not straightforwardly known, this definition can be unclear, and the general approach is to leave the cell uninterrupted for significant time to achieve thermodynamic equilibrium. However, the cell is often not left to rest to full thermodynamic equilibrium during use while calculating the OCV [45]. In practice, the OCV is calculated from the cell potential once a plateau occurs in the cell potential over time.

Alternatively, the OCV can be calculated from the activity of the electrochemically active components within the cell. This can allow the OCV dependency on behavior to be substituted with their molarities or concentrations. This approach requires the use of activity coefficients for the active components within the cell, which are generally found by simplified assumptions of ideal active components due to the lack of readily available data from a functioning cell. This simplification may in some cases lead to OCV estimation errors [46]. In terms of LIBs in electric vehicles, the only parameters measured are generally the current, voltage and temperature of the cell; therefore, the method used for OCV determination is based on the former method requiring thermodynamic equilibrium.

Using the OCV is highly precise and simple method for SoC estimation. The connection between SoC and OCV is extracted from the stepwise calculation of OCV for various SoC values in a LIB. An example of this connection is given in Figure 3. Despite this, the OCV and SoC relationship for each LIB varies over the battery life and the related hysteresis effect, while they are of the same rating, content, and structure [47,48]. The value of OCVs is not the same when charging and discharging due to hysteresis characteristics, despite having the same SoC value [49]. The main drawback is it takes time to reach thermodynamic equilibrium conditions, which makes it only applicable when the vehicle is at rest, instead of in driving mode. It has been shown that it is possible to estimate the OCV of a redox flow battery without waiting to reach equilibrium conditions [44]; however, this has not yet been shown in LIBs. In previous years, the literature has suggested numerous updated OCV-based methods to improve processing time and accuracy [50,51]. However, this approach is inadequate for SoC estimation due to its strong reliance on the OCV, the requirement for equilibrium conditions and precision calculation of charging/discharging voltages [47].

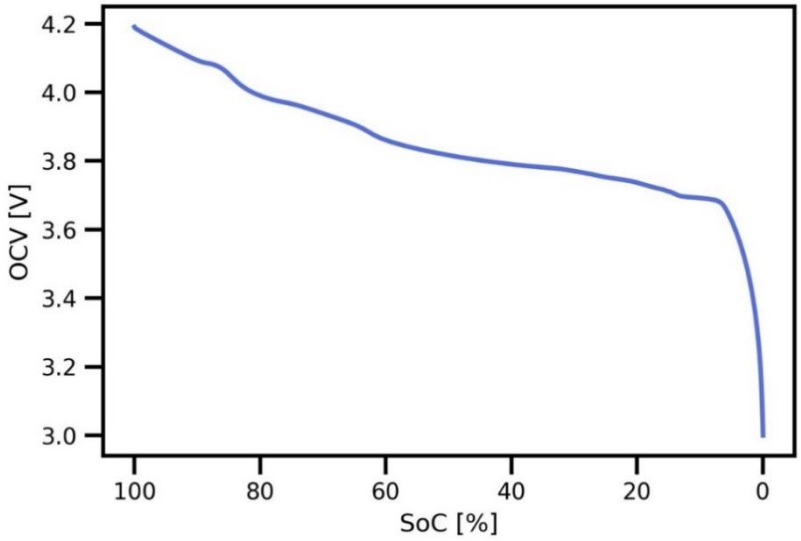

Figure 3. The relationship of the open circuit voltage with the state-of-charge. The OCV of a Lithium cobalt oxide (LCO) battery produced by Melasta Battery (Model No. SLPBB042126HN) with a capacity of 6550 mAh. The battery was cycled in an Arbin Instruments cycler at 25 °C. The OCV was estimated from cycling at a c-rate of c/20, and the SoC was estimated using the coulomb counting method.

3.1.3. State of Health

Generally, when calculating the SoC, the rated, real, or cycle capacity is used for C_a (Equation (4)) [52–54]. Therefore, defining the established battery capacity is not consistent [55]. In the theoretical analysis, capacity is used as the equation denominator, treating C_a as a fixed number, and the SoC is calculated by deducting the charge sum from C_a [56]. An important parameter to consider then is the SoH, which is the ratio of maximum residual capacity at the time (C_m) to the maximum available capacity of the battery when new (Equation (5)).

$$\mathrm{SoH}(t) = \left(\frac{C_m}{C_a}\right) \cdot 100\% \tag{5}$$

SoH allows the inclusion of BEV LIB ageing and is affected by different causes (e.g., driving style and ambient temperature). Owing to the effect of various LIB fluctuations (e.g., temperature), the inconsistencies of battery voltage, internal resistance, and power can increase to some extent, influencing the value of SoH. Therefore, it is vital to consider the relationship between SoH, SoC, and depth-of-discharge (DoD).

$$\mathrm{SoC}(t) = \mathrm{SoH}(t) - \mathrm{DoD}(t) \tag{6}$$

Here, DoD is expressed as the percentage of capacity that can be discharged relative to the available capacity (i.e., $\left(\frac{C_m - C_r}{C_a}\right) \cdot 100\%$).

3.2. Estimation of Energy and Remaining Capacity

Physically, a LIB discharge transfers Li from the anode to the cathode, with the opposite occurring during charging. Electrochemically, the SoC is positively associated to the Li concentration in the anode and negatively to the Li concentration in the cathode. The cell potential depends on the concentration of the electrode surface, where SoC depends on average concentration of particles, making SoC estimation using the potential challenging. Another aspect is determining the amount energy in a LIB pack. This is essential for battery electric vehicles, as the calculated vehicle range is entirely dependent on this. Therefore, the state-of-energy (SoE; residual energy) calculation is vital.

3.2.1. Look-Up Tables

Look-up tables are useful and forthright, allowing SoC estimation through mapping the connection between characteristic parameters of the LIB and the SoC [57]. The primary drawback of look-up tables is that the LIB must be resting for a long time for reliability of the internal electrochemistry, so that measurements can be precise. SoC calculation efficiency also relies dramatically on the precision of the table used. Therefore, the approach is not suitable for online and precise estimation of SoC.

Open-Circuit Voltage

The OCV is the LIB potential after a long, load-free rest, and has a nonlinear relationship with SoC [58,59]. Comprehensive methods have been presented where the OCV is calculated for various SoC levels producing extensive OCV-SoC tables [58,59]. The process is straightforward; however, the LIB must rest for significant time to ensure accurate OCV measurement. Considering the effect of temperature, substance, driving style, and aging on the OCV-SoC relationship, these considerations must be applied to the OCV-SoC table [60]. An OCV-SoC-temperature table has been developed to infer SoC battery [61]. The hysteresis effect is also an important factor impacting the accuracy [62–64]. An incorrect OCV-SoC correlation deprived of understanding of the hysteresis effect will lead to incorrect SoC estimations.

Impedance

A relationship concerning impedance and SoC also exists. By adding a current frequency to the battery, the nonlinear fitting or parameter recognition algorithm can determine multiple SoC-related parameters (e.g., internal ohmic resistance), and then an impedance look-up table method can be used [65,66]. However, battery ageing can influence the precision of the SoC look-up table process and can cause substantial predictive errors [67]. Moreover, current and ambient temperature can contribute to non-linear impedance and SoC changes [68].

3.2.2. Ampere-Hour Integral

Ampere-hour integral is a simpler method where current integration is used for SoC estimation [69]; however, this is at the cost of some clear disadvantages. Sensor error can occur due to the open-loop estimation, which will produce large errors in the SoC estimation. Additionally, deviations in Coulomb performance can materialize from temperature and aging, also affecting the accuracy of SoC estimation. Furthermore, the initial SoC is estimated using look-up tables, so preliminary errors will propagate through the entire estimation process. This approach is typically paired with model-based or data-driven methods to improve its sturdiness.

3.2.3. Filter-Based

The model-based estimators can usually be loosely clustered into Bayesian estimators (filters), deterministic observers, and learning algorithms. The compared performances of these estimation methods in this section mainly depend on the individual models that are used with the estimation method rather than the standalone estimation method itself.

Most common Bayesian estimators are the variants of Kalman filters. Recently, a number of alternatives are used to estimate SoC in LIBs with Kalman filters (Figure 4).

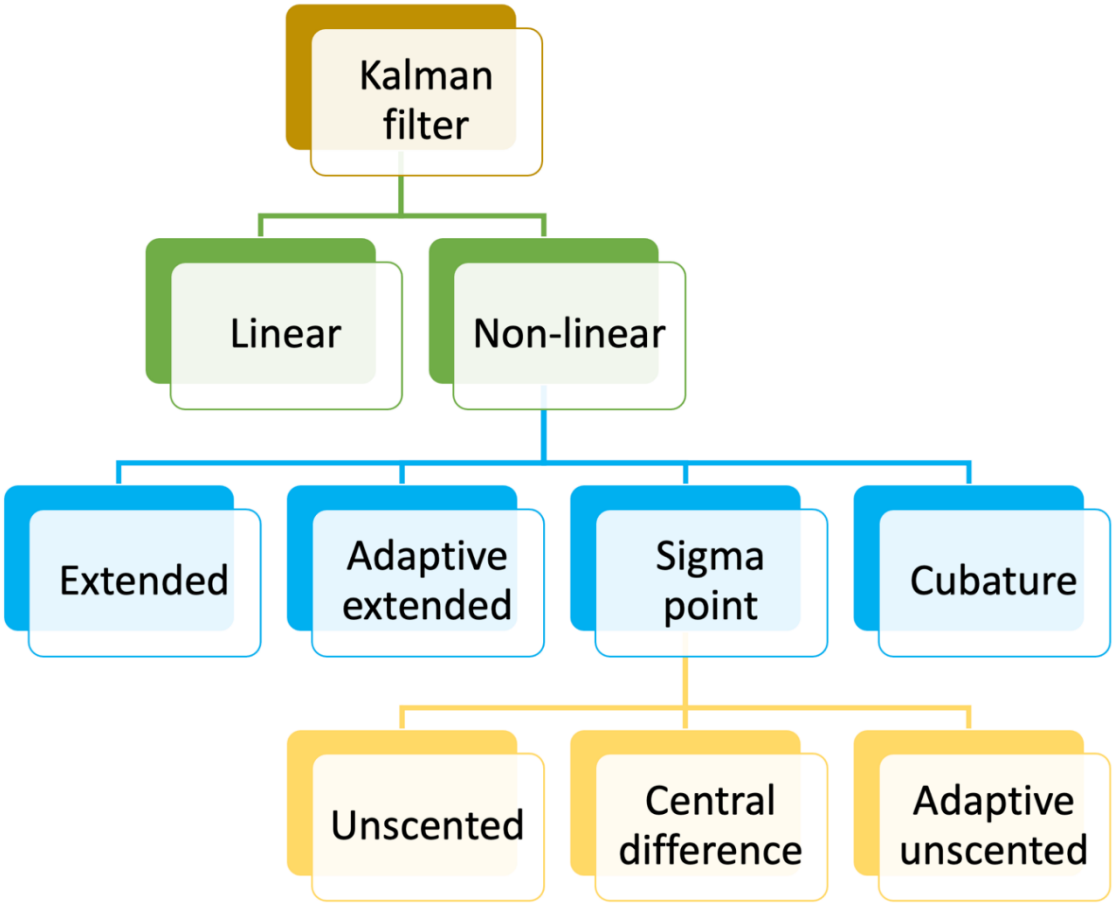

Figure 4. The Kalman filter family of algorithms that have been used for state-of-charge estimation in battery electric vehicle Lithium-ion batteries.

Linear Kalman Filter

The Kalman filter has been commonly used for BEV LIB SoC estimation [70]. The general estimation algorithm can be regarded as a recursive mechanism involving first the estimating the system states, and second updating the system states based on the feedback errors [71]. Linear Kalman filter is optimal for linear systems. As the OCV is nonlinear, Kalman filters cannot be used explicitly for OCV-based estimations [72]. The OCV function can be linearized with local linearization, optimizing Kalman filters for SoC estimation [73].

Extended Kalman Filter

The theory of the extended Kalman filter is to linearize the nonlinear system at each time step [74]. When used with OCV-based models, it extends the nonlinear OCV function with partial derivatives based on the nonlinear function linearization principle [75]. As model parameters are easily modified due to nonlinear behavior, an SoC estimation approach based on a reduced-order LIB model and an extended Kalman filter has been proposed with errors below 2% [76]. Alternatively, SoC estimation of a LIB based on a dual-time scale extended Kalman filter has been developed, where the average SoC was measured for all cells, then the individual cell SoC was calculated by the discrepancy between the mean and each individual cell [77]. This yielded an SoC error below 2%. Overall, the extended Kalman filter's accuracy depends not only on OCV function linearization, but on the model parameters also [78]; as a consequence, improved approaches can be classified into either model improvement of algorithm improvement [10].

Adaptive Extended Kalman Filter

When the parameters or the noise covariances of any Kalman filter are adapted according to the measurements, it is called an adaptive Kalman filter. He et al. used an adaptive extended Kalman filter for estimating SoC, where the process and measurement noise covariances are adapted [79]. This helps the adaptive extended Kalman filter effectively prevent algorithm divergence or bias [80,81]. Based on a closed-loop feedback system with multiparameter input, an adaptive extended Kalman filter calculated the correct SoC estimate with a median SoC error of 3% [82]; however, this did not take LIB aging into account. To upgrade the battery-aging model, a basic optimization algorithm can be applied, and an adaptive extended Kalman filter can calculate the SoC in aging LIBs with an error of less than 4% [83]. As the fractional-order model provides a clearer explanation of LIB behavior, the adaptive extended Kalman filter estimates the SoC using the fractional-order model [84].

Sigma-Point Kalman Filter

A sigma-point Kalman filter supplements the extended Kalman filter where the nonlinear component is overlooked. Therefore, sigma-point Kalman filter SoC estimation has been suggested [85], and an electrochemical model-based SoC estimation approach was proposed using an adaptive square root sigma point Kalman filter with equality constraints observing a 30% improvement compared to an adaptive extended Kalman filter [86].

Unscented Kalman Filter

The unscented Kalman filter is a nonlinear estimator and is developed from traceless transformation. Nonlinear machine formulas can be extended to regular Kalman filter by unscented transformation [87]. The unscented Kalman filters transformation does not neglect higher-order terms, but it has high precision estimates [88]. To improve conventional unscented Kalman filter performance, several improved algorithms have been produced [89]. To minimize computational requirements for unscented transformation in the unscented Kalman filter, the square root unscented Kalman spherical transform filter was developed to estimate battery SoC [90]; however, the maximum error increased by 37% compared to extended Kalman filters. The Fuzzy Inference System was used to improve the robustness and simplify the unscented Kalman filter [91], where the SoC error was reported to be below 1.76%.

Adaptive Unscented Kalman Filter

Sun et al. have estimated SoC of a LIB using an adaptive unscented Kalman filters where the noise covariance is auto tuned [92]. A recursive least-square approach defined on-line model parameters and modified the adaptive unscented Kalman filter state model in real-time, minimizing the SoC estimate error [93]. When comparing adaptive unscented, adaptive extended, unscented, and extended Kalman filters performance in SoC estimates based on a second order resistor-capacitor model, the adaptive unscented Kalman filters achieved the best results [94]. Other experimental results have also found that SoC prediction accuracy is better with adaptive unscented Kalman filters when compared to unscented Kalman filters and extended Kalman filters [95,96].

Central Difference Kalman Filter

This method uses the Sterling interpolation formula to generate the Sigma points, which then finds the posterior distribution of the states [97]. It has been shown that the central different Kalman filter was efficient than the extended Kalman filter at determining the SoC [98,99].

Cubature Difference Kalman Filter

The cubature difference Kalman filter uses the spherical-radial cubature rule to calculate the multivariate moment integrals. It is centered on the radial volume criterion of the

third-order, where the cubature difference Kalman filter approximates the average value of the nonlinear state using a sequence of volume coordinates that can efficiently resolve the difficulty of nonlinear state estimation [100]. Two important steps are to turn the integral form into the spherical integral form and the spherical radial third-order criterion. It has been observed that the cubature difference Kalman filter error in SoC estimation is 1.78% lower than that of extended Kalman filter approaches [101]; however, the estimation time is significantly extended.

Particle Filter

Unlike the Kalman filter variants described earlier, the particle filter is based on probability densities, thus can handle non-Gaussian systems. When designing a particle filter, the main difficulty is to select the proper proposal distributions that can approximate the posterior distributions. The most common method is to use the transition prior for this. The particle filters central concept is to produce a series of independent random sampling points in the state space according to the system state vector's scalar distribution, then change the particle location and state to the detected values. The maximal particle state is then estimated by changing particle sets [102,103]. Results have demonstrated the particle filters are much better than extended Kalman filters in estimating the SoC [104–107].

Unscented Particle Filter

Using the transition prior as a proposal distribution in particle filters can be inefficient, if new measurements appear at the tail of the prior (when there are abrupt changes in measurement data) or if the likelihood is narrow and high compared to the prior (when sensors are highly precise). To avoid this problem, usually extended Kalman filter approximation or unscented Kalman filter approximation is used as the proposal distribution of the particle filter. When the unscented Kalman filter approximation is used, the particle filter is called an unscented particle filter. The unscented particle filter is an improved particle filter, where the key concept is to boost the particle filter sampling. Calculation results provide online observation detail, improving the particle filter sampling effect [108]. The unscented particle filter has been widely used in SoC estimation due to its superior efficiency [109,110], with SoC estimation errors below 2% at a high computational efficiency [111].

Cubature Particle Filter

Cubature particle filter is based on spherical-radial cubature rule of the third degree and generally used in high-dimensional state estimations. The third-degree cubature rule is a special form of the unscented transformation but with a higher numerical stability. However, both the unscented and cubature particle filters have limitations in both accuracy and robustness. Cubature particle filters measure the average and discrepancy of a nonlinear random function by the volume method explicitly and produces the proposed density function for weighted particles. By then measuring the particle mean, the minimum mean square error approximation is obtained [112]. The cubature particle filter algorithm uses the new measurement knowledge when producing particles, improving the degree of approximation of the later likelihood of machine state [113]. The cubature particle filter has been observed to outperform the extended particle filter in terms of errors; however, the computational efficiency is low [114]. By using an adaptive weighted cubature particle filter, the computational efficiency was improved and the error in SoC estimation was reduced to 1% [115].

3.2.4. Observer-Based

Although the observer is a common term that is used for any type of estimator including the Bayesian filters or learning algorithms, the observer mentioned in this section refers only to the deterministic observers. This includes classical Luenberger type observers, finite-dimensional observers, and combined observers. To realize state input or

other control system requirements, state observer definition and construction processes have been suggested [116]. Recently, observer-based approaches (e.g., the Luenberger observer) have been commonly used to estimate the necessary states of LIBs.

Luenberger

The Luenberger observer is used extensively in linear, nonlinear, and time-varying systems [117]. Hu et al. [118] suggested an adaptive Luenberger observer system for online LIB pack SoC estimation, where the observer gain was adapted using a stochastic gradient approach. A nonlinear fractional LIB model-based SoC estimation has also been developed using a Luenberger observer [119], where the global asymptotic stability is ensured using a direct Lyapunov method.

Sliding Mode

Sliding mode observers are mainly used in LIB estimation where disturbances and measurement noise have sufficiently large switching gains [120]. Built from the sliding mode controller, the sliding mode observer retains robust tracking efficiency under model instabilities and environmental interferences [120]. A second-order discrete-time sliding mode observer has been implemented to eradicate what is known as the chattering phenomenon [121]. Furthermore, an adaptive gain sliding mode observer was proposed to minimize chattering levels and the compensate for errors in the model [122,123]. Moreover, a Gray prediction-based fuzzy sliding mode observer, which is combined with fuzzy logic, has been suggested to both minimize chattering and overcome overestimation [124]. Here, the battery voltage value was calculated by grey estimation and the gains on the sliding mode observer were calibrated through the fuzzy inference system to forecast the error. A combined neural network-based robust sliding mode observer has also been proposed with an adaptive switching gain to mitigate chattering effects in a lithium polymer battery [122,123]. Here, a radial-based neural network is integrated to the observer to ensure the convergence of SoC estimation errors [125].

Proportional Integral

A proportional-integral observer is a combined observer of proportional and integral observers and is an effective way of calculating the states with uncertain input disturbance. A parameter-normalized proportional integral observer was devised to manage the power error and initial error in LIB measurements, and the new integrator was to confine the drifting current effect. It was observed that this approach had lower computational complexity but high precision without matrix operation, even though the original SoC was uncertain [126].

H-Infinity

The H-infinity observer will ensure robustness of the incorrect initial state and uncertain disruption when imprecise or unidentified statistical characteristics from modelling and calculating errors are present. When combining an H-infinity observer with a hysteresis model, it may be possible to accommodate model ambiguities from temperature, aging and current [127]. A dynamic gain H-infinity observer has also been developed for battery pack SoC estimation, which can decrease the adverse impact of non-Gaussian models and measurement errors [128,129].

3.2.5. Data-Driven

Data-driven approaches presume the LIB is a black box model and learn internal dynamics by vast quantities of measured data. The main data-driven estimation methods used in LIB estimation include genetic algorithms, support vector machines, and neural networks and are usually used together with another estimation or inference method. For an extensive overview of data-driven methods that can be applied to SoC estimation in LIBs, the authors suggest the recent articles by Lipu et al. [130] and Vidal et al. [131].

Genetic Algorithm

Usually, a genetic algorithm is used to define the parameters of a LIB for further SoC estimation [132]. A novel SoC estimation approach focused on a sliding mode Gray model which is combined with genetic algorithm has been developed, where the use of genetic algorithm introduced greater precision and repeatability [133].

Support Vector Machines

A support vector machine is a cluster of supervised learning methods that can use kernels for various number of learning tasks [133,134]. As support vector machines are based on the structural risk minimization principle, it can perform better than the conventional neural networks. However, the increasing modelling size and the single output structure are disadvantages of this method [132]. An improved support vector machine for regression-based SoC estimation process has been suggested, where the observed results suggested it was a straightforward and reliable method compared to artificial neural networks [135]. Alternatively, adaptive unscented Kalman filters and least-square support vector machines were integrated to approximate battery SoC, where, even with minimal training samples, the LIB model can be correctly developed and modified [136].

Artificial Neural Networks

The neural network approach (Figure 5) has outstanding potential to form a nonlinear map showing an intricate nonlinear model [137]. An OCV-based SoC calculation based on the dual neural network fusion LIB model, where the linear neural network LIB model was used to define first-order or second-order electrochemical model parameters, and the second back-propagation neural network was used to take the OCV-to-SoC relationship [138]. A further development in back-propagation neural networks resulted in a strategy that utilizes principal component analysis and particle swarm optimization allowing improved accuracy and robustness of the estimation [139].

A radial basis function neural network-based uncertainty quantification algorithm has also been developed to build a response surface approximate model to estimate a multi-cell LIB pack SoC, as used in BEVs [140]. A novel approach based on a deep feed-forward neural network was used for LIB SoC estimation, by directly mapping the measurements to the SoC [141]. By establishing a load-classifying neural network model to estimate SoC, overfitting of the model was suppressed as a result of the model structure and the postprocessing [137]. A nonlinear observer based on a radial basis function neural network has also been proposed [142], which used an inclusive equivalent circuit model.

Lipu et al. [143] established a nonlinear autoregressive with exogenous input-based neural network that was optimized for the field of SoC estimation, where the lightning search algorithm allowed the identification for the optimal input delays, feedback delays and hidden layer neurons. Recently, Hannan et al. [144] presented a recurrent nonlinear autoregressive with exogenous inputs neural network with using the lightning search algorithm to increase SoC estimation. This further developed the approach by allowing accurate SoC estimation under different LIB conditions. By using the Levenberg–Marquardt-optimized multi-hidden layer wavelet neural network model proposed by Xia et al. [145], SoC estimation was possible through particle swarm optimization.

A stacked long short-term memory recurrent neural network was established to model LIB dynamics and estimate the SoC, with the approach providing rapid estimation to the true SoC, despite the original SoC being incorrect [146]. A similar approach was recently published where transfer learning was exploited to accelerate the neural network training, with a rolling learning method developed to implement SoH influence [147]. This method yielded precise estimation under different conditions, allowing a well-trained model to be straightforwardly transferred to similar battery chemistries. Further advancements were made by Chen et al. [148], where an autoregressive long short-term memory network and moving horizon estimation were used for SoC estimation. This method was investigated to

assess whether it was a suitable approach for SoC estimation when there is uncertainty or large deviations from the initial SoC.

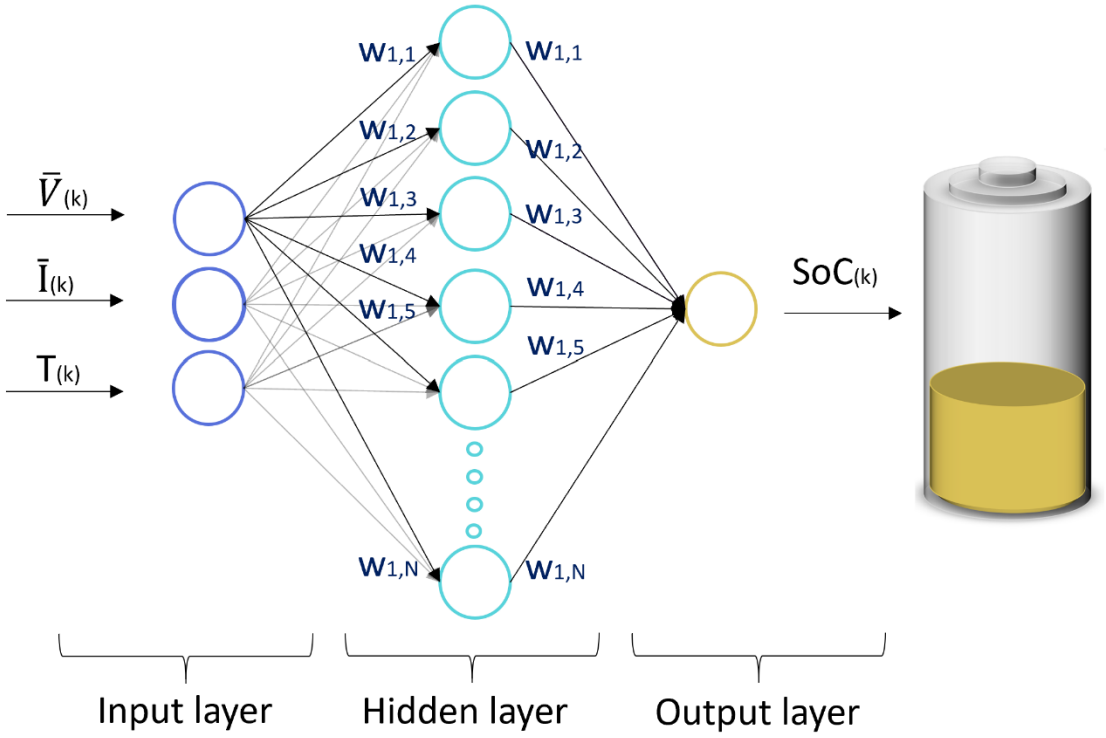

Figure 5. Architecture of a generalized feedforward neural network of voltage (V), current (I), and time (T) inputs, a double layer and nodes where W is the weights, and the state-of-charge (SoC) output.

3.3. Comparison of Approaches

The look-up table approach is straightforward and can map the nonlinear relationship between the SoC and OCV; however, it cannot meet real-time specifications due to the variability of the OCV during operation and is vulnerable to sensor imprecision. The ampere-hour integral approach is also rather straightforward and does not require high-cost computational resources; however, the precision depends largely on the determination of the original SoC and sensor accuracy. The ampere-hour integral approach, together with OCV look-up table or model-based methods, are promising approaches to acquire improved accuracy of SoC estimation in LIBs.

Filter-based and observer-based methods (examples of model-based approaches) can achieve high precision SoC estimation. Despite this, the accuracy of model-based methods depends on the accuracy of the model itself; therefore, extensive computational resources are required as the algorithms within such approaches are complex. Similarly, the type of estimator that can be used also depends on the type of model and the state space system that is used, which makes the comparison of estimators difficult, therefore general remarks are used.

Kalman filter-based approaches are commonly used in calculating SoC in LIBs. The linear Kalman filter-based approach only suits linear structures; however, the extended Kalman filter approach can overcome this as it applies a linearization approximation to nonlinear systems to address this. Despite this, the extended Kalman filter approaches' performance is unstable in terms of linearization error, making it unfit for high-order non-linear processes as seen in SoC in BEV LIBs. The sigma-point and unscented Kalman filter methods are used for SoC estimation in order to avoid complicated Jacobian matrix and Gaussian noise computation; however, significant computational resources are required to perform such approaches when the number of states/parameters are high. In order to

overcome this, adaptive methods (e.g., adaptive extended and adaptive unscented Kalman filters) have been developed to improve the robustness of the method against measurement and process noise. The particle filter approach is proposed to manage non-Gaussian systems and has shown high precision. More specifically, the unscented and cubature Kalman filter approaches are designed to enhance the process of particle sampling and estimate the likelihood of the state; however, in such approaches, the convergence rate remains a problem.

Observer-based approaches can also achieve adequate estimate precision against unprecise sensor data or initial state errors; however, problems still exist for the determination of the appropriate gain. Data-driven models are dissimilar to model-based approaches and are insensitive to the performance of the model and external environmental factors. The key pitfalls are that these approaches typically entail high computational cost and long processing time, and the precision depends largely on the training data used. Table 1 gives an overview of the mentioned methods for estimating SoC in LIBs.

Table 1. The comparison of SoC estimation methods for LiBs.

	Method	**Maximum Error ($\leq \pm$)**
Look-up tables	OCV	1.2% [58]
	Impedance	1.4% [66]
Ampere-hour integral	Current integration	4% [69]
Filter	Linear Kalman	2% [72]
	Extended Kalman	1.4% [74]
	Adaptive Kalman	2% [80]
	Sigma-point Kalman	1.2% [85]
	Unscented Kalman	0.12% [87]
	Adaptive unscented Kalman	0.1% [94]
	Central difference Kalman	1.4% [98]
	Cubature Kalman	2.7% [101]
	Particle	0.86% [106]
	Unscented particle	0.9% [114]
	Cubature particle	1.1% [114]
Observer	Luenberger	0.88% [118]
	Sliding mode	2% [120]
	Proportional integral	2.5% [126]
	H-infinity	3.36% [128]
Data-driven	Genetic algorithm	2.98% [33]
	Support vector machine	6% [134]
	Neural network	3.8% [137]

3.4. Errors in Modeling

When implementing model-based SoC estimation, the errors caused by numerous sources and their consequence on estimation should be contemplated. Error amassing directly affects precision and convergence rate of SoC estimation. There are six types of errors that can be caused, such as ampere-hour counting and voltage-based correction when SoC is estimated using a nonlinear observer for a second-order equivalent circuit model (Figure 6) [146]. Hardware and software selection plays a crucial role in SoC estimation and should include high-precision sensors, good power approximation algorithms, and a highly accurate LIB modeling approach to reduce the impact of accumulating various errors.

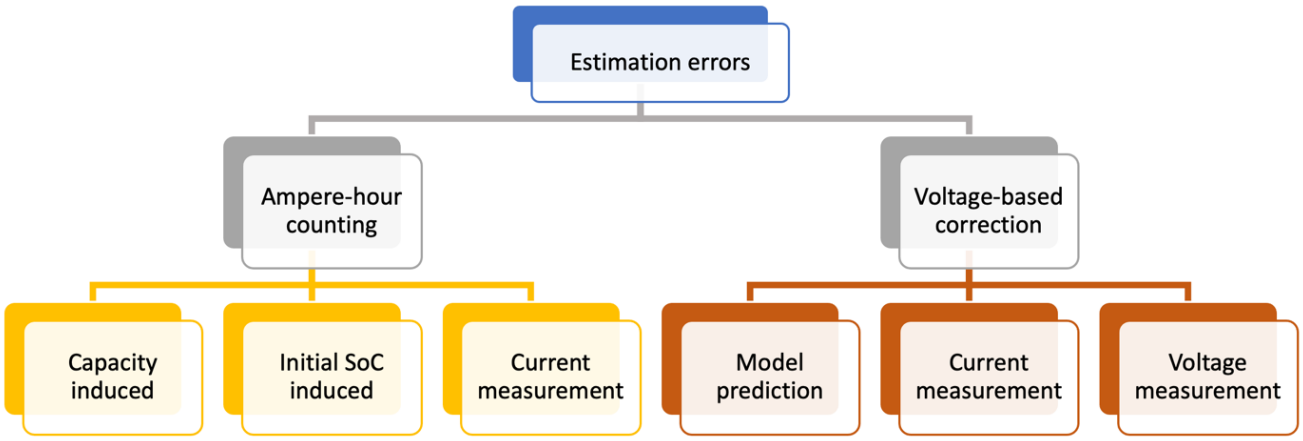

Figure 6. Sources of errors in model-based approaches to state-of-charge estimation in battery electric vehicle Lithium-ion batteries.

3.4.1. Capacity Induced Errors

The decline in capacity observed in aging LIBs is responsible for capacity induced errors in SoC modeling; however, this can be minimized during estimation by updating the LIB capacity within the model. For example, use of Kalman filter algorithms for SoC estimation can significantly reduce the effect of capacity induced errors during dynamic loading [149]. Furthermore, when a highly accurate battery model is used, capacity induced SoC errors can be reduced [150].

3.4.2. Initial SoC Error

Initial SoC error is the discrepancy between the actual initial SoC and the initial SoC estimate. To initialize the calculation, the first iteration requires initial SoC error to provide the initial SoC. The initial SoC value can be acquired from the look-up table or the current saved SoC value. Due to the recursive update of Kalman filter gain during estimation [149], the initial SoC error value is decreased and almost removed within the initial iterations. The initial SoC error converges rapidly to zero with significant observer gain [150].

3.4.3. Current Measurement Error

Measured current is fed to the ampere-hour counting and voltage-based rectification, both potentially developing current measurement error. Current measurement error is largely triggered by low current sensor accuracy, bias error, and noise produced during measurement. The noise impact on SoC errors is marginal due to integration in ampere-hour counting methods. Typically, the current measurement error produced in ampere-hour counting is unidirectional and can expand in the first iterations of the model [149]. The current measurement error produced in voltage-based correction is contrary to the current measurement error caused in ampere-hour counting [150]. Therefore, due to the current measurement error created by ampere-hour counting, the observer gain escalates and the comprehensive eradication of the error could be achievable within numerous iterations of the model [150].

3.4.4. Model Prediction Error

Model prediction error indicates to the variance among the estimated model output (potential in the model) and actual output (actual potential in the model) and has a significant contribution to SoC estimation error. Model prediction error can be separated into two segments, bias error, and noise. Model potential noise does not adversely disturb SoC estimation and accuracy [149]; however, the model prediction error's high dependence on the OCV-to-SoC association is a perplexing problem for SoC estimation using Kalman filter algorithms [150].

3.4.5. Voltage Measurement Error

Voltage measurement error can also occur as a consequence of bias and noise error. The noise error depends on the environment and is difficult to estimate; however, the most estimation algorithms can proficiently quash noise [150]. Bias error can be produced by the discrepancies in actual voltage and measured voltage of the LIB. To counteract this bias defect, the model can fabricate voltage divergence processes [149].

4. Challenges in SoC Estimation in LiBs

With the popularization of BEV LIB storage technologies, innovative control technology has grown in interest. It is difficult to correctly model the LIB structure and predict the condition, which significantly affects BMS efficiency and effectiveness. Research in specific areas is still required to obtain advanced BMS systems.

4.1. Advanced Optical Fiber Sensing

The internal states and parameters are hard to calculate directly within a LIB using traditional sensor methods. Although LIB state estimation algorithms exist, there is still room for calculation and parameter recognition errors. Therefore, contemporary sensor technologies are required to directly measure internal parameters of the BEV LIB. Optical fiber technology is one such method for determining internal measurements of LIB parameters [151–161]. These can be directly embedded within the LIB to measure temperature and strain [162–164], where the latter could improve SoC estimation. Optical fiber sensor technology is expected to enhance battery management, with future research aimed to develop real-time, reliable, and stable sensors merged with multisensor data fusion tools to achieve better knowledge of the LIBs internal state.

4.2. Multi-State Estimation

The single-state estimation approach is well researched; however, there is potential for the BEV LIB state to be nonuniform, which leads to errors in SoC estimation with the current approach. Multi-state estimation may provide a useful approach to account for multiple states within the BEV LIB [165–167]. These approaches have dramatically increased the SoC, voltage and power estimation precision. This area of research in BEV LIB SoC is still in its early stages of development, but it is a promising path for future progress in SoC estimation.

4.3. Battery Model Selection and Estimated Parameter Accuracy

Different LIB types retain their features in differing circumstances; however, owing to the intricate electrochemical behavior in complex conditions, model choice for SoC estimation becomes difficult. Model complexity is also an important aspect, largely based on the amount of model factors that are required to be defined. For selecting the ideal SoC estimation algorithm, the compromise amongst simplicity and accuracy is a vital parameter.

4.4. Operating Conditions

Model-based SoC estimation accuracy is significantly affected by the heterogeneity of BEV LIB model features, and the relationship between OCV and SoC induced by temperature, c-rate, and SoC range [168–170]. It has been observed that the internal resistance of a LIB is impartial to the effective SoC range when using various external temperature environments. Model parameter values are extremely temperature sensitive, but affected by the c-rate and SoC range to a lesser extent. Alternatively, the OCV-to-SoC association remains consistent with varying external working conditions (Figure 7). Despite this, when the SoC is below 10%, the OCV will lead to significant errors in SoC estimation. For BEV LIBs used in varying operating conditions, changes in temperature and c-rate (e.g., driving style and charging rate) are high, making the variation of the model parameters more significant. For reliable SoC prediction in such applications, the model parameters must also be revised online [171–173].

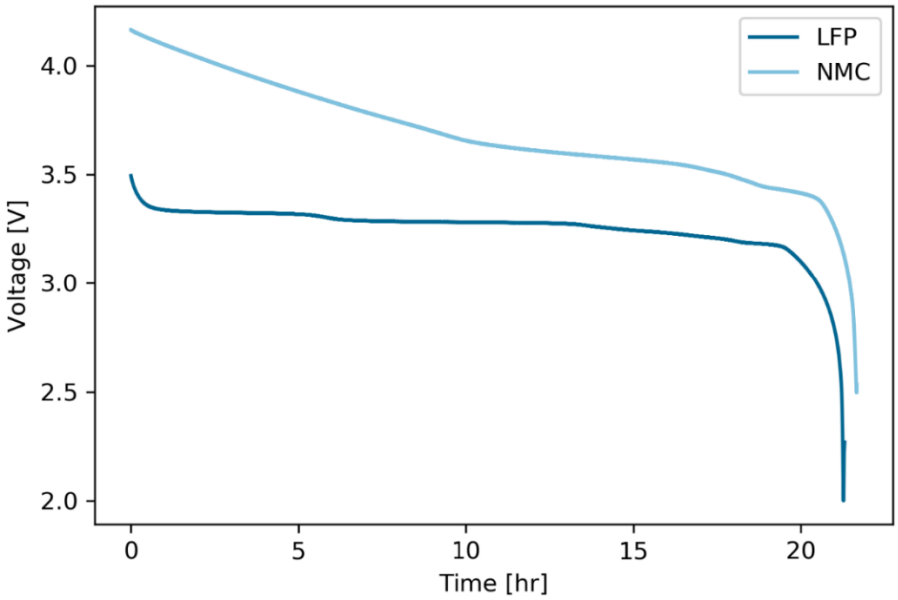

Figure 7. The decreasing voltage of two common LIB chemistries during discharge. The battery data were obtained from in [174] using low C-rate discharge (C/22), allowing the terminal voltage to be used to approximate the OCV.

5. Conclusions

This review has presented the physical properties that outline SoC in BEV LIBs. Current and voltage are the main physical parameters used in order to estimate the SoC in BEV LIBs. These can be straightforwardly used with physical electrochemical, data-driven models, and electrical equivalent models in order to estimate the SoC, with the latter two models being routinely used in LIB SoC estimation in BEVs. However, the accuracy of these approaches is low, and this can become a concern in optimal monitoring of the LIB state.

The alternative is to use state estimation methods based on look-up tables, ampere hour integrals, filter-based, observer-based, or data-driven estimation algorithms to determine the state. These methods allow a higher accuracy in state estimation for LIBs, but still produce some error. They also can require significant computational power, resulting in significant time in order to acquire the estimated state.

In order to improve SoC estimation, research should focus on optimization of estimation approaches that allow SoC estimation without significant computational power. Additionally, focus should be directed towards reducing the error accumulation by improving the fundamental understanding of battery function. By focusing on capacity induced error, initial SoC error, current measurement error, and voltage measurement error, the error in the model estimation should be minimized. This could allow the use of less demanding algorithms with smaller errors. In order to achieve this, many challenges are required to be overcome. Such challenges could be alleviated with use of internal optical fiber sensing, multi-state estimation, estimated model parameter accuracy, and operating conditions. Overall, there is still significant progress to be made in this area of research, but the convergence point is getting closer.

Funding: This research received no external funding.

Institutional Review Board Statement: Not applicable.

Informed Consent Statement: Not applicable.

Acknowledgments: The authors acknowledge the support from the ENERSENSE research initiative, NTNU, Norway. The authors also acknowledge Freyr Battery AS, NTNU (Project No. 90492503) and EIT Innoenergy SE (Project No. 02-2019-IP172-FREYR).

Conflicts of Interest: The authors declare no conflict of interest.

References

1. Rahimi-Eichi, H.; Ojha, U.; Baronti, F.; Chow, M.-Y. Battery management system: An overview of its application in the smart grid and electric vehicles. *IEEE Ind. Electron. Mag.* **2013**, *7*, 4–16. [CrossRef]
2. Felius, L.C.; Lamb, J.J.; Hrynyszyn, B.D.; Dessen, F. Smart components and systems. In *Energy-Smart Buildings: Design, Construction and Monitoring of Buildings for Improved Energy Efficiency*; IOP Publishing: Bristol, UK, 2020; Volume 1, pp. 1–16.
3. Lamb, J.J.; Pollet, B.G.; Burheim, O.S. Energy storage. In *Energy-Smart Buildings Design: Construction and Monitoring of Buildings for Improved Energy Efficiency*; IOP Publishing: Bristol, UK, 2020; Volume 1, pp. 1–14.
4. Hamre, B.; Bracchi, T.; Felius, L.C.; Burheim, O.S.; Pollet, B.G.; Lamb, J.J. Energy production in buildings. In *Energy-Smart Buildings: Design, Construction and Monitoring of Buildings for Improved Energy Efficiency*; IOP Publishing: Bristol, UK, 2020; Volume 1, pp. 1–13.
5. Aaldering, L.J.; Leker, J.; Song, C.H. Analysis of technological knowledge stock and prediction of its future development potential: The case of lithium-ion batteries. *J. Clean. Prod.* **2019**, *223*, 301–311. [CrossRef]
6. Feng, X.; Ouyang, M.; Liu, X.; Lu, L.; Xia, Y.; He, X. Thermal runaway mechanism of lithium ion battery for electric vehicles: A review. *Energy Storage Mater.* **2018**, *10*, 246–267. [CrossRef]
7. Hu, X.; Cao, D.; Egardt, B. Condition monitoring in advanced battery management systems: Moving horizon estimation using a reduced electrochemical model. *IEEE/ASME Trans. Mechatron.* **2017**, *23*, 167–178. [CrossRef]
8. Chaturvedi, N.A.; Klein, R.; Christensen, J.; Ahmed, J.; Kojic, A. Algorithms for advanced battery-management systems. *IEEE Control Syst. Mag.* **2010**, *30*, 49–68.
9. Wang, Y.; Chen, Z.; Zhang, C. On-line remaining energy prediction: A case study in embedded battery management system. *Appl. Energy* **2017**, *194*, 688–695. [CrossRef]
10. Wang, Y.; Tian, J.; Sun, Z.; Wang, L.; Xu, R.; Li, M.; Chen, Z. A comprehensive review of battery modeling and state estimation approaches for advanced battery management systems. *Renew. Sustain. Energy Rev.* **2020**, *131*, 110015. [CrossRef]
11. Zhang, Q.; Wang, D.; Yang, B.; Cui, X.; Li, X. Electrochemical model of lithium-ion battery for wide frequency range applications. *Electrochim. Acta* **2020**, *34*, 136094. [CrossRef]
12. Nejad, S.; Gladwin, D.T.; Stone, D.A. A systematic review of lumped-parameter equivalent circuit models for real-time estimation of lithium-ion battery states. *J. Power Sources* **2016**, *316*, 183–196. [CrossRef]
13. Seaman, A.; Dao, T.-S.; McPhee, J. A survey of mathematics-based equivalent-circuit and electrochemical battery models for hybrid and electric vehicle simulation. *J. Power Sources* **2014**, *256*, 410–423. [CrossRef]
14. Wei, J.; Dong, G.; Chen, Z. Remaining useful life prediction and state of health diagnosis for lithium-ion batteries using particle filter and support vector regression. *IEEE Trans. Ind. Electron.* **2017**, *65*, 5634–5643. [CrossRef]
15. Wang, Y.; Yang, D.; Zhang, X.; Chen, Z. Probability based remaining capacity estimation using data-driven and neural network model. *J. Power Sources* **2016**, *315*, 199–208. [CrossRef]
16. Romero-Becerril, A.; Alvarez-Icaza, L. Comparison of discretization methods applied to the single-particle model of lithium-ion batteries. *J. Power Sources* **2011**, *196*, 10267–10279. [CrossRef]
17. Grandjean, T.R.B.; Li, L.; Odio, M.X.; Widanage, W.D. Global Sensitivity Analysis of the Single Particle Lithium-Ion Battery Model with Electrolyte. In Proceedings of the 2019 IEEE Vehicle Power and Propulsion Conference (VPPC), Hanoi, Vietnam, 14–17 October 2019; IEEE: Piscataway, NJ, USA, 2019; pp. 1–7.
18. Doyle, M.; Fuller, T.F.; Newman, J. Modeling of galvanostatic charge and discharge of the lithium/polymer/insertion cell. *J. Electrochem. Soc.* **1993**, *140*, 1526. [CrossRef]
19. Dao, T.-S.; Vyasarayani, C.P.; McPhee, J. Simplification and order reduction of lithium-ion battery model based on porous-electrode theory. *J. Power Sources* **2012**, *198*, 329–337. [CrossRef]
20. Han, X.; Ouyang, M.; Lu, L.; Li, J. Simplification of physics-based electrochemical model for lithium ion battery on electric vehicle. Part II: Pseudo-two-dimensional model simplification and state of charge estimation. *J. Power Sources* **2015**, *278*, 814–825. [CrossRef]
21. Guo, X.; Kang, L.; Yao, Y.; Huang, Z.; Li, W. Joint estimation of the electric vehicle power battery state of charge based on the least squares method and the Kalman filter algorithm. *Energies* **2016**, *9*, 100. [CrossRef]
22. Johnson, V.H. Battery performance models in ADVISOR. *J. Power Sources* **2002**, *110*, 321–329. [CrossRef]
23. Liaw, B.Y.; Nagasubramanian, G.; Jungst, R.G.; Doughty, D.H. Modeling of lithium ion cells—A simple equivalent-circuit model approach. *Solid State Ion.* **2004**, *175*, 835–839.
24. Verbrugge, M.; Tate, E. Adaptive state of charge algorithm for nickel metal hydride batteries including hysteresis phenomena. *J. Power Sources* **2004**, *126*, 236–249. [CrossRef]
25. Wang, Y.; Liu, C.; Pan, R.; Chen, Z. Modeling and state-of-charge prediction of lithium-ion battery and ultracapacitor hybrids with a co-estimator. *Energy* **2017**, *121*, 739–750. [CrossRef]

26. Zhang, X.; Lu, J.; Yuan, S.; Yang, J.; Zhou, X. A novel method for identification of lithium-ion battery equivalent circuit model parameters considering electrochemical properties. *J. Power Sources* **2017**, *345*, 21–29. [CrossRef]
27. Brand, J.; Zhang, Z.; Agarwal, R.K. Extraction of battery parameters of the equivalent circuit model using a multi-objective genetic algorithm. *J. Power Sources* **2014**, *247*, 729–737. [CrossRef]
28. Gao, P.; Zhang, C.; Wen, G. Equivalent circuit model analysis on electrochemical impedance spectroscopy of lithium metal batteries. *J. Power Sources* **2015**, *294*, 67–74. [CrossRef]
29. Jang, J.; Yoo, J. Equivalent circuit evaluation method of lithium polymer battery using bode plot and numerical analysis. *IEEE Trans. Energy Convers.* **2011**, *26*, 290–298. [CrossRef]
30. Freeborn, T.J.; Maundy, B.; Elwakil, A.S. Fractional-order models of supercapacitors, batteries and fuel cells: A survey. *Mater. Renew. Sustain. Energy* **2015**, *4*, 9. [CrossRef]
31. Yang, Q.; Xu, J.; Cao, B.; Li, X. A simplified fractional order impedance model and parameter identification method for lithium-ion batteries. *PLoS ONE* **2017**, *12*, e0172424. [CrossRef]
32. Zou, Y.; Li, S.E.; Shao, B.; Wang, B. State-space model with non-integer order derivatives for lithium-ion battery. *Appl. Energy* **2016**, *161*, 330–336. [CrossRef]
33. Mu, H.; Xiong, R.; Zheng, H.; Chang, Y.; Chen, Z. A novel fractional order model based state-of-charge estimation method for lithium-ion battery. *Appl. Energy* **2017**, *207*, 384–393. [CrossRef]
34. Xiong, R.; Tian, J.; Shen, W.; Sun, F. A novel fractional order model for state of charge estimation in lithium ion batteries. *IEEE Trans. Veh. Technol.* **2018**, *68*, 4130–4139. [CrossRef]
35. Wang, Q.-K.; He, Y.-J.; Shen, J.-N.; Ma, Z.-F.; Zhong, G.-B. A unified modeling framework for lithium-ion batteries: An artificial neural network based thermal coupled equivalent circuit model approach. *Energy* **2017**, *138*, 118–132. [CrossRef]
36. Zhang, C.; Zhu, Y.; Dong, G.; Wei, J. Data-driven lithium-ion battery states estimation using neural networks and particle filtering. *Int. J. Energy Res.* **2019**, *43*, 8230–8241. [CrossRef]
37. Thangavel, V.; Guerrero, O.X.; Quiroga, M.; Mikala, A.M.; Rucci, A.; Franco, A.A. A three dimensional kinetic Monte Carlo model for simulating the carbon/sulfur mesostructural evolutions of discharging lithium sulfur batteries. *Energy Storage Mater.* **2020**, *24*, 472–485. [CrossRef]
38. Shrivastava, P.; Soon, T.K.; Idris, M.Y.I.B.; Mekhilef, S. Overview of model-based online state-of-charge estimation using Kalman filter family for lithium-ion batteries. *Renew. Sustain. Energy Rev.* **2019**, *113*, 109233. [CrossRef]
39. Kim, I.-S. Nonlinear state of charge estimator for hybrid electric vehicle battery. *IEEE Trans. Power Electron.* **2008**, *23*, 2027–2034.
40. Plett, G.L. Extended Kalman filtering for battery management systems of LiPB-based HEV battery packs: Part 3. State and parameter estimation. *J. Power Sources* **2004**, *134*, 277–292. [CrossRef]
41. Feng, F.; Lu, R.; Zhu, C. A combined state of charge estimation method for lithium-ion batteries used in a wide ambient temperature range. *Energies* **2014**, *7*, 3004–3032. [CrossRef]
42. Meissner, E.; Richter, G. Battery monitoring and electrical energy management: Precondition for future vehicle electric power systems. *J. Power Sources* **2003**, *116*, 79–98. [CrossRef]
43. Zhang, C.; Jiang, J.; Zhang, L.; Liu, S.; Wang, L.; Loh, P.C. A generalized SOC-OCV model for lithium-ion batteries and the SOC estimation for LNMCO battery. *Energies* **2016**, *9*, 900. [CrossRef]
44. Del Olmo, D.; Pavelka, M.; Kosek, J. Open-Circuit Voltage Comes from Non-Equilibrium Thermodynamics. *J. Non-Equilib. Thermodyn.* **2020**, *46*, 91–108. [CrossRef]
45. Vágner, P.; Kodým, R.; Bouzek, K. Thermodynamic analysis of high temperature steam and carbon dioxide systems in solid oxide cells. *Sustain. Energy Fuels* **2019**, *3*, 2076–2086. [CrossRef]
46. Pavelka, M.; Wandschneider, F.; Mazur, P. Thermodynamic derivation of open circuit voltage in vanadium redox flow batteries. *J. Power Sources* **2015**, *293*, 400–408. [CrossRef]
47. Lee, S.; Kim, J.; Lee, J.; Cho, B.H. State-of-charge and capacity estimation of lithium-ion battery using a new open-circuit voltage versus state-of-charge. *J. Power Sources* **2008**, *185*, 1367–1373. [CrossRef]
48. Cuma, M.U.; Koroglu, T. A comprehensive review on estimation strategies used in hybrid and battery electric vehicles. *Renew. Sustain. Energy Rev.* **2015**, *42*, 517–531. [CrossRef]
49. Hannan, M.A.; Lipu, M.S.H.; Hussain, A.; Mohamed, A. A review of lithium-ion battery state of charge estimation and management system in electric vehicle applications: Challenges and recommendations. *Renew. Sustain. Energy Rev.* **2017**, *78*, 834–854. [CrossRef]
50. Waag, W.; Sauer, D.U. Adaptive estimation of the electromotive force of the lithium-ion battery after current interruption for an accurate state-of-charge and capacity determination. *Appl. Energy* **2013**, *111*, 416–427. [CrossRef]
51. Leng, F.; Tan, C.M.; Yazami, R.; Le, M.D. A practical framework of electrical based online state-of-charge estimation of lithium ion batteries. *J. Power Sources* **2014**, *255*, 423–430. [CrossRef]
52. Dincer, I.; Hamut, H.S.; Javani, N. *Thermal Management of Electric Vehicle Battery Systems*; John Wiley & Sons: Hoboken, NJ, USA, 2016; ISBN 1118900219.
53. Andrea, D. *Battery Management Systems for Large Lithium Ion Battery Packs*; Artech House: Norwood, MA, USA, 2010; ISBN 1608071057.
54. Rahn, C.D.; Wang, C.-Y. *Battery Systems Engineering*; John Wiley & Sons: Hoboken, NJ, USA, 2013; ISBN 1118517059.

55. Lillehei, C.W.; Cruz, A.B.; Johnsrude, I.; Sellers, R.D. A new method of assessing the state of charge of implanted cardiac pacemaker batteries. *Am. J. Cardiol.* **1965**, *16*, 717–721. [CrossRef]
56. Tan, X. *Electric Vehicle Power Battery Management System Design*; Sun Yat-sen University Press: Guangzhou, China, 2011.
57. How, D.N.T.; Hannan, M.A.; Lipu, M.S.H.; Ker, P.J. State of charge estimation for lithium-ion batteries using model-based and data-driven methods: A review. *IEEE Access* **2019**, *7*, 136116–136136. [CrossRef]
58. Pop, V.; Bergveld, H.J.; het Veld, J.H.G.O.; Regtien, P.P.L.; Danilov, D.; Notten, P.H.L. Modeling battery behavior for accurate state-of-charge indication. *J. Electrochem. Soc.* **2006**, *153*, A2013. [CrossRef]
59. Ali, M.U.; Zafar, A.; Nengroo, S.H.; Hussain, S.; Junaid Alvi, M.; Kim, H.-J. Towards a smarter battery management system for electric vehicle applications: A critical review of lithium-ion battery state of charge estimation. *Energies* **2019**, *12*, 446. [CrossRef]
60. Klintberg, A.; Zou, C.; Fridholm, B.; Wik, T. Kalman filter for adaptive learning of two-dimensional look-up tables applied to OCV-curves for aged battery cells. *Control Eng. Pract.* **2019**, *84*, 230–237. [CrossRef]
61. Xing, Y.; He, W.; Pecht, M.; Tsui, K.L. State of charge estimation of lithium-ion batteries using the open-circuit voltage at various ambient temperatures. *Appl. Energy* **2014**, *113*, 106–115. [CrossRef]
62. Dong, G.; Wei, J.; Zhang, C.; Chen, Z. Online state of charge estimation and open circuit voltage hysteresis modeling of LiFePO4 battery using invariant imbedding method. *Appl. Energy* **2016**, *162*, 163–171. [CrossRef]
63. Ovejas, V.J.; Cuadras, A. Effects of cycling on lithium-ion battery hysteresis and overvoltage. *Sci. Rep.* **2019**, *9*, 1–9. [CrossRef] [PubMed]
64. Rashid, M.; Pathan, T.S.; McGordon, A.; Kendrick, E.; Widanage, W.D. Investigation of hysteresis and relaxation behaviour in graphite and LiNi0. 33Mn0. 33Co0. 33O2 electrodes. *J. Power Sources* **2019**, *440*, 227153. [CrossRef]
65. Zheng, L.; Zhang, L.; Zhu, J.; Wang, G.; Jiang, J. Co-estimation of state-of-charge, capacity and resistance for lithium-ion batteries based on a high-fidelity electrochemical model. *Appl. Energy* **2016**, *180*, 424–434. [CrossRef]
66. Bao, Y.; Dong, W.; Wang, D. Online internal resistance measurement application in lithium ion battery capacity and state of charge estimation. *Energies* **2018**, *11*, 1073. [CrossRef]
67. Huet, F.; Nogueira, R.P.; Lailler, P.; Torcheux, L. Investigation of the high-frequency resistance of a lead-acid battery. *J. Power Sources* **2006**, *158*, 1012–1018. [CrossRef]
68. Huang, W.; Qahouq, J.A.A. An online battery impedance measurement method using DC–DC power converter control. *IEEE Trans. Ind. Electron.* **2014**, *61*, 5987–5995. [CrossRef]
69. Zhang, Y.; Song, W.; Lin, S.; Feng, Z. A novel model of the initial state of charge estimation for LiFePO4 batteries. *J. Power Sources* **2014**, *248*, 1028–1033. [CrossRef]
70. Xu, L.; Wang, J.; Chen, Q. Kalman filtering state of charge estimation for battery management system based on a stochastic fuzzy neural network battery model. *Energy Convers. Manag.* **2012**, *53*, 33–39. [CrossRef]
71. Mastali, M.; Vazquez-Arenas, J.; Fraser, R.; Fowler, M.; Afshar, S.; Stevens, M. Battery state of the charge estimation using Kalman filtering. *J. Power Sources* **2013**, *239*, 294–307. [CrossRef]
72. Dong, G.; Wei, J.; Chen, Z. Kalman filter for onboard state of charge estimation and peak power capability analysis of lithium-ion batteries. *J. Power Sources* **2016**, *328*, 615–626. [CrossRef]
73. Yu, Z.; Huai, R.; Xiao, L. State-of-charge estimation for lithium-ion batteries using a kalman filter based on local linearization. *Energies* **2015**, *8*, 7854–7873. [CrossRef]
74. Xiong, R.; Sun, F.; Chen, Z.; He, H. A data-driven multi-scale extended Kalman filtering based parameter and state estimation approach of lithium-ion polymer battery in electric vehicles. *Appl. Energy* **2014**, *113*, 463–476. [CrossRef]
75. Chen, Z.; Fu, Y.; Mi, C.C. State of charge estimation of lithium-ion batteries in electric drive vehicles using extended Kalman filtering. *IEEE Trans. Veh. Technol.* **2012**, *62*, 1020–1030. [CrossRef]
76. Lee, J.; Nam, O.; Cho, B.H. Li-ion battery SOC estimation method based on the reduced order extended Kalman filtering. *J. Power Sources* **2007**, *174*, 9–15. [CrossRef]
77. Dai, H.; Wei, X.; Sun, Z.; Wang, J.; Gu, W. Online cell SOC estimation of Li-ion battery packs using a dual time-scale Kalman filtering for EV applications. *Appl. Energy* **2012**, *95*, 227–237. [CrossRef]
78. Lee, K.-T.; Dai, M.-J.; Chuang, C.-C. Temperature-compensated model for lithium-ion polymer batteries with extended Kalman filter state-of-charge estimation for an implantable charger. *IEEE Trans. Ind. Electron.* **2017**, *65*, 589–596. [CrossRef]
79. He, H.; Xiong, R.; Zhang, X.; Sun, F.; Fan, J. State-of-charge estimation of the lithium-ion battery using an adaptive extended Kalman filter based on an improved Thevenin model. *IEEE Trans. Veh. Technol.* **2011**, *60*, 1461–1469.
80. Xiong, R.; He, H.; Sun, F.; Zhao, K. Evaluation on state of charge estimation of batteries with adaptive extended Kalman filter by experiment approach. *IEEE Trans. Veh. Technol.* **2012**, *62*, 108–117. [CrossRef]
81. He, H.; Xiong, R.; Guo, H. Online estimation of model parameters and state-of-charge of LiFePO4 batteries in electric vehicles. *Appl. Energy* **2012**, *89*, 413–420. [CrossRef]
82. Xiong, R.; Gong, X.; Mi, C.C.; Sun, F. A robust state-of-charge estimator for multiple types of lithium-ion batteries using adaptive extended Kalman filter. *J. Power Sources* **2013**, *243*, 805–816. [CrossRef]
83. Sepasi, S.; Ghorbani, R.; Liaw, B.Y. A novel on-board state-of-charge estimation method for aged Li-ion batteries based on model adaptive extended Kalman filter. *J. Power Sources* **2014**, *245*, 337–344. [CrossRef]
84. Zhu, Q.; Xu, M.; Liu, W.; Zheng, M. A state of charge estimation method for lithium-ion batteries based on fractional order adaptive extended kalman filter. *Energy* **2019**, *187*, 115880. [CrossRef]

85. Seo, B.-H.; Nguyen, T.H.; Lee, D.-C.; Lee, K.-B.; Kim, J.-M. Condition monitoring of lithium polymer batteries based on a sigma-point Kalman filter. *J. Power Electron.* **2012**, *12*, 778–786. [CrossRef]
86. Bi, Y.; Choe, S.-Y. An adaptive sigma-point Kalman filter with state equality constraints for online state-of-charge estimation of a Li (NiMnCo) O2/Carbon battery using a reduced-order electrochemical model. *Appl. Energy* **2020**, *258*, 113925. [CrossRef]
87. Zhang, J.; Xia, C. State-of-charge estimation of valve regulated lead acid battery based on multi-state Unscented Kalman Filter. *Int. J. Electr. Power Energy Syst.* **2011**, *33*, 472–476. [CrossRef]
88. Chen, Z.; Yang, L.; Zhao, X.; Wang, Y.; He, Z. Online state of charge estimation of Li-ion battery based on an improved unscented Kalman filter approach. *Appl. Math. Model.* **2019**, *70*, 532–544. [CrossRef]
89. Gholizade-Narm, H.; Charkhgard, M. Lithium-ion battery state of charge estimation based on square-root unscented Kalman filter. *IET Power Electron.* **2013**, *6*, 1833–1841. [CrossRef]
90. Aung, H.; Low, K.S.; Goh, S.T. State-of-charge estimation of lithium-ion battery using square root spherical unscented Kalman filter (Sqrt-UKFST) in nanosatellite. *IEEE Trans. Power Electron.* **2014**, *30*, 4774–4783. [CrossRef]
91. Zeng, M.; Zhang, P.; Yang, Y.; Xie, C.; Shi, Y. SOC and SOH Joint Estimation of the Power Batteries Based on Fuzzy Unscented Kalman Filtering Algorithm. *Energies* **2019**, *12*, 3122. [CrossRef]
92. Sun, F.; Hu, X.; Zou, Y.; Li, S. Adaptive unscented Kalman filtering for state of charge estimation of a lithium-ion battery for electric vehicles. *Energy* **2011**, *36*, 3531–3540. [CrossRef]
93. Liu, G.; Xu, C.; Li, H.; Jiang, K.; Wang, K. State of charge and online model parameters co-estimation for liquid metal batteries. *Appl. Energy* **2019**, *250*, 677–684. [CrossRef]
94. Partovibakhsh, M.; Liu, G. An adaptive unscented Kalman filtering approach for online estimation of model parameters and state-of-charge of lithium-ion batteries for autonomous mobile robots. *IEEE Trans. Control Syst. Technol.* **2014**, *23*, 357–363. [CrossRef]
95. Peng, S.; Chen, C.; Shi, H.; Yao, Z. State of charge estimation of battery energy storage systems based on adaptive unscented Kalman filter with a noise statistics estimator. *IEEE Access* **2017**, *5*, 13202–13212. [CrossRef]
96. Qiu, X.; Guo, Y.; Zhang, J.; Zhao, H.; Peng, X.; Wu, Z.; Tian, R.; Yang, J. State of Charge Estimation of Lithium Battery Energy Storage Systems Based on Adaptive Correntropy Unscented Kalman Filter. In Proceedings of the 2020 5th Asia Conference on Power and Electrical Engineering (ACPEE), Chengdu, China, 4–7 June 2020; IEEE: Piscataway, NJ, USA, 2020; pp. 851–857.
97. Lim, J. CDKF approach for estimating a static parameter of carrier frequency offset based on nonlinear measurement equations in OFDM systems. *Nonlinear Dyn.* **2014**, *78*, 703–711. [CrossRef]
98. Xuan, D.-J.; Shi, Z.; Chen, J.; Zhang, C.; Wang, Y.-X. Real-time estimation of state-of-charge in lithium-ion batteries using improved central difference transform method. *J. Clean. Prod.* **2020**, *252*, 119787. [CrossRef]
99. Sangwan, V.; Kumar, R.; Rathore, A.K. State-of-charge estimation for li-ion battery using extended Kalman filter (EKF) and central difference Kalman filter (CDKF). In Proceedings of the 2017 IEEE Industry Applications Society Annual Meeting, Cincinnati, OH, USA, 14 March 2018; IEEE: Piscataway, NJ, USA, 2017; pp. 1–6.
100. Arasaratnam, I.; Haykin, S. Cubature kalman filters. *IEEE Trans. Automat. Contr.* **2009**, *54*, 1254–1269. [CrossRef]
101. Peng, J.; Luo, J.; He, H.; Lu, B. An improved state of charge estimation method based on cubature Kalman filter for lithium-ion batteries. *Appl. Energy* **2019**, *253*, 113520. [CrossRef]
102. Nummiaro, K.; Koller-Meier, E.; Van Gool, L. An adaptive color-based particle filter. *Image Vis. Comput.* **2003**, *21*, 99–110. [CrossRef]
103. Tulsyan, A.; Tsai, Y.; Gopaluni, R.B.; Braatz, R.D. State-of-charge estimation in lithium-ion batteries: A particle filter approach. *J. Power Sources* **2016**, *331*, 208–223. [CrossRef]
104. Chen, Z.; Sun, H.; Dong, G.; Wei, J.; Wu, J.I. Particle filter-based state-of-charge estimation and remaining-dischargeable-time prediction method for lithium-ion batteries. *J. Power Sources* **2019**, *414*, 158–166. [CrossRef]
105. Schwunk, S.; Armbruster, N.; Straub, S.; Kehl, J.; Vetter, M. Particle filter for state of charge and state of health estimation for lithium–iron phosphate batteries. *J. Power Sources* **2013**, *239*, 705–710. [CrossRef]
106. Wang, Y.; Zhang, C.; Chen, Z. A method for state-of-charge estimation of LiFePO4 batteries at dynamic currents and temperatures using particle filter. *J. Power Sources* **2015**, *279*, 306–311. [CrossRef]
107. Liu, X.; Chen, Z.; Zhang, C.; Wu, J. A novel temperature-compensated model for power Li-ion batteries with dual-particle-filter state of charge estimation. *Appl. Energy* **2014**, *123*, 263–272. [CrossRef]
108. Van Der Merwe, R.; Doucet, A.; De Freitas, N.; Wan, E. The unscented particle filter. *Adv. Neural Inf. Process. Syst.* **2000**, *13*, 584–590.
109. He, Y.; Liu, X.; Zhang, C.; Chen, Z. A new model for State-of-Charge (SOC) estimation for high-power Li-ion batteries. *Appl. Energy* **2013**, *101*, 808–814. [CrossRef]
110. Wang, Y.; Chen, Z. A framework for state-of-charge and remaining discharge time prediction using unscented particle filter. *Appl. Energy* **2020**, *260*, 114324. [CrossRef]
111. Shen, Y. Hybrid unscented particle filter based state-of-charge determination for lead-acid batteries. *Energy* **2014**, *74*, 795–803. [CrossRef]
112. Wang, D.; Yang, F.; Tsui, K.-L.; Zhou, Q.; Bae, S.J. Remaining useful life prediction of lithium-ion batteries based on spherical cubature particle filter. *IEEE Trans. Instrum. Meas.* **2016**, *65*, 1282–1291. [CrossRef]

113. Guo, R.; Gan, Q.; Zhang, J.; Guo, K.; Dong, J. Huber cubature particle filter and online state estimation. *Proc. Inst. Mech. Eng. Part I J. Syst. Control Eng.* **2017**, *231*, 158–167. [CrossRef]
114. Xia, B.; Sun, Z.; Zhang, R.; Cui, D.; Lao, Z.; Wang, W.; Sun, W.; Lai, Y.; Wang, M. A comparative study of three improved algorithms based on particle filter algorithms in soc estimation of lithium ion batteries. *Energies* **2017**, *10*, 1149. [CrossRef]
115. Zhang, K.; Ma, J.; Zhao, X.; Zhang, D.; He, Y. State of Charge Estimation for Lithium Battery Based on Adaptively Weighting Cubature Particle Filter. *IEEE Access* **2019**, *7*, 166657–166666. [CrossRef]
116. Luenberger, D. An introduction to observers. *IEEE Trans. Automat. Contr.* **1971**, *16*, 596–602. [CrossRef]
117. Luenberger, D. Observers for multivariable systems. *IEEE Trans. Automat. Contr.* **1966**, *11*, 190–197. [CrossRef]
118. Hu, X.; Sun, F.; Zou, Y. Estimation of state of charge of a lithium-ion battery pack for electric vehicles using an adaptive Luenberger observer. *Energies* **2010**, *3*, 1586–1603. [CrossRef]
119. Wang, B.; Liu, Z.; Li, S.E.; Moura, S.J.; Peng, H. State-of-charge estimation for lithium-ion batteries based on a nonlinear fractional model. *IEEE Trans. Control Syst. Technol.* **2016**, *25*, 3–11. [CrossRef]
120. Huangfu, Y.; Xu, J.; Zhao, D.; Liu, Y.; Gao, F. A novel battery state of charge estimation method based on a super-twisting sliding mode observer. *Energies* **2018**, *11*, 1211. [CrossRef]
121. Kim, D.; Koo, K.; Jeong, J.J.; Goh, T.; Kim, S.W. Second-order discrete-time sliding mode observer for state of charge determination based on a dynamic resistance li-ion battery model. *Energies* **2013**, *6*, 5538–5551. [CrossRef]
122. Chen, X.; Shen, W.; Cao, Z.; Kapoor, A. Adaptive gain sliding mode observer for state of charge estimation based on combined battery equivalent circuit model. *Comput. Chem. Eng.* **2014**, *64*, 114–123. [CrossRef]
123. Chen, X.; Shen, W.; Cao, Z.; Kapoor, A. A novel approach for state of charge estimation based on adaptive switching gain sliding mode observer in electric vehicles. *J. Power Sources* **2014**, *246*, 667–678. [CrossRef]
124. Kim, D.; Goh, T.; Park, M.; Kim, S.W. Fuzzy sliding mode observer with grey prediction for the estimation of the state-of-charge of a lithium-ion battery. *Energies* **2015**, *8*, 12409–12428. [CrossRef]
125. Chen, X.; Shen, W.; Dai, M.; Cao, Z.; Jin, J.; Kapoor, A. Robust adaptive sliding-mode observer using RBF neural network for lithium-ion battery state of charge estimation in electric vehicles. *IEEE Trans. Veh. Technol.* **2015**, *65*, 1936–1947. [CrossRef]
126. Tang, X.; Wang, Y.; Chen, Z. A method for state-of-charge estimation of LiFePO4 batteries based on a dual-circuit state observer. *J. Power Sources* **2015**, *296*, 23–29. [CrossRef]
127. Xie, J.; Ma, J.; Sun, Y.; Li, Z. Estimating the state-of-charge of lithium-ion batteries using an H-infinity observer with consideration of the hysteresis characteristic. *J. Power Electron.* **2016**, *16*, 643–653. [CrossRef]
128. Zhu, Q.; Xiong, N.; Yang, M.-L.; Huang, R.-S.; Hu, G.-D. State of charge estimation for lithium-ion battery based on nonlinear observer: An H∞ method. *Energies* **2017**, *10*, 679. [CrossRef]
129. Zhu, Q.; Li, L.; Hu, X.; Xiong, N.; Hu, G.-D. H_∞-Based Nonlinear Observer Design for State of Charge Estimation of Lithium-Ion Battery With Polynomial Parameters. *IEEE Trans. Veh. Technol.* **2017**, *66*, 10853–10865. [CrossRef]
130. Lipu, M.S.H.; Hannan, M.A.; Hussain, A.; Ayob, A.; Saad, M.H.M.; Karim, T.F.; How, D.N.T. Data-driven state of charge estimation of lithium-ion batteries: Algorithms, implementation factors, limitations and future trends. *J. Clean. Prod.* **2020**, *277*, 124110. [CrossRef]
131. Vidal, C.; Malysz, P.; Kollmeyer, P.; Emadi, A. Machine Learning Applied to Electrified Vehicle Battery State of Charge and State of Health Estimation: State-of-the-Art. *IEEE Access* **2020**, *8*, 52796–52814. [CrossRef]
132. Ting, T.O.; Man, K.L.; Lim, E.G.; Leach, M. Tuning of Kalman filter parameters via genetic algorithm for state-of-charge estimation in battery management system. *Sci. World J.* **2014**, *2014*, 176052. [CrossRef] [PubMed]
133. Chen, L.; Wang, Z.; Lü, Z.; Li, J.; Ji, B.; Wei, H.; Pan, H. A novel state-of-charge estimation method of lithium-ion batteries combining the grey model and genetic algorithms. *IEEE Trans. Power Electron.* **2017**, *33*, 8797–8807. [CrossRef]
134. Anton, J.C.A.; Nieto, P.J.G.; Viejo, C.B.; Vilán, J.A.V. Support vector machines used to estimate the battery state of charge. *IEEE Trans. Power Electron.* **2013**, *28*, 5919–5926. [CrossRef]
135. Hu, J.N.; Hu, J.J.; Lin, H.B.; Li, X.P.; Jiang, C.L.; Qiu, X.H.; Li, W.S. State-of-charge estimation for battery management system using optimized support vector machine for regression. *J. Power Sources* **2014**, *269*, 682–693. [CrossRef]
136. Meng, J.; Luo, G.; Gao, F. Lithium polymer battery state-of-charge estimation based on adaptive unscented Kalman filter and support vector machine. *IEEE Trans. Power Electron.* **2015**, *31*, 2226–2238. [CrossRef]
137. Tong, S.; Lacap, J.H.; Park, J.W. Battery state of charge estimation using a load-classifying neural network. *J. Energy Storage* **2016**, *7*, 236–243. [CrossRef]
138. Dang, X.; Yan, L.; Xu, K.; Wu, X.; Jiang, H.; Sun, H. Open-circuit voltage-based state of charge estimation of lithium-ion battery using dual neural network fusion battery model. *Electrochim. Acta* **2016**, *188*, 356–366. [CrossRef]
139. Hossain Lipu, M.S.; Hannan, M.A.; Hussain, A.; Saad, M.H.M. Optimal BP neural network algorithm for state of charge estimation of lithium-ion battery using PSO with PCA feature selection. *J. Renew. Sustain. Energy* **2017**, *9*, 64102. [CrossRef]
140. Sun, F.; Xiong, R.; He, H. A systematic state-of-charge estimation framework for multi-cell battery pack in electric vehicles using bias correction technique. *Appl. Energy* **2016**, *162*, 1399–1409. [CrossRef]
141. Chemali, E.; Kollmeyer, P.J.; Preindl, M.; Emadi, A. State-of-charge estimation of Li-ion batteries using deep neural networks: A machine learning approach. *J. Power Sources* **2018**, *400*, 242–255. [CrossRef]
142. Chen, J.; Ouyang, Q.; Xu, C.; Su, H. Neural network-based state of charge observer design for lithium-ion batteries. *IEEE Trans. Control Syst. Technol.* **2017**, *26*, 313–320. [CrossRef]

143. Lipu, M.S.H.; Hannan, M.A.; Hussain, A.; Saad, M.H.M.; Ayob, A.; Blaabjerg, F. State of charge estimation for lithium-ion battery using recurrent NARX neural network model based lighting search algorithm. *IEEE Access* **2018**, *6*, 28150–28161. [CrossRef]
144. Hannan, M.A.; Lipu, M.S.H.; Hussain, A.; Ker, P.J.; Mahlia, T.M.I.; Mansor, M.; Ayob, A.; Saad, M.H.; Dong, Z.Y. Toward enhanced State of charge estimation of Lithium-ion Batteries Using optimized Machine Learning techniques. *Sci. Rep.* **2020**, *10*, 1–15.
145. Xia, B.; Cui, D.; Sun, Z.; Lao, Z.; Zhang, R.; Wang, W.; Sun, W.; Lai, Y.; Wang, M. State of charge estimation of lithium-ion batteries using optimized Levenberg-Marquardt wavelet neural network. *Energy* **2018**, *153*, 694–705. [CrossRef]
146. Yang, F.; Song, X.; Xu, F.; Tsui, K.-L. State-of-charge estimation of lithium-ion batteries via long short-term memory network. *IEEE Access* **2019**, *7*, 53792–53799. [CrossRef]
147. Liu, Y.; Shu, X.; Yu, H.; Shen, J.; Zhang, Y.; Liu, Y.; Chen, Z. State of charge prediction framework for lithium-ion batteries incorporating long short-term memory network and transfer learning. *J. Energy Storage* **2021**, *37*, 102494. [CrossRef]
148. Chen, Y.; Li, C.; Chen, S.; Ren, H.; Gao, Z. A combined robust approach based on auto-regressive long short-term memory network and moving horizon estimation for state-of-charge estimation of lithium-ion batteries. *Int. J. Energy Res.* **2021**. [CrossRef]
149. Zheng, Y.; Ouyang, M.; Han, X.; Lu, L.; Li, J. Investigating the error sources of the online state of charge estimation methods for lithium-ion batteries in electric vehicles. *J. Power Sources* **2018**, *377*, 161–188. [CrossRef]
150. Shen, P.; Ouyang, M.; Han, X.; Feng, X.; Lu, L.; Li, J. Error analysis of the model-based state-of-charge observer for lithium-ion batteries. *IEEE Trans. Veh. Technol.* **2018**, *67*, 8055–8064. [CrossRef]
151. Wahl, M.S.; Lamb, J.J.; Muri, H.I.; Snilsberg, R.K.; Hjelme, D.R. Light properties and sensors. In *Micro-Optics and Energy: Sensors for Energy Devices.*; Springer: Berlin/Heidelberg, Germany, 2020.
152. Muri, H.I.; Wahl, M.S.; Lamb, J.J.; Snilsberg, R.K.; Hjelme, D.R. Sensor fusion. In *Micro-Optics and Energy: Sensors for Energy Devices*; Springer International Publishing: New York, NY, USA, 2020.
153. Spitthoff, L.; Lamb, J.J.; Pollet, B.; Burheim, O.S. Lifetime expectancy of lithium-ion batteries. In *Micro-Optics and Energy: Sensors for Energy Devices*; Springer: Berlin/Heidelberg, Germany, 2020.
154. Spitthoff, L.; Øyre, E.S.; Muri, H.I.; Wahl, M.S.; Gunnarshaug, A.F.; Pollet, B.; Lamb, J.J.; Burheim, O.S. Thermal management of Lithium ion batteries. In *Micro-Optics and Energy: Sensors for Energy Devices*; Springer International Publishing: New York, NY, USA, 2020.
155. Wahl, M.S.; Muri, H.I.; Snilsberg, R.K.; Lamb, J.J.; Hjelme, D.R. Temperature and humidity measurements. In *Micro-Optics and Energy: Sensors for Energy Devices*; Springer International Publishing: New York, NY, USA, 2020.
156. Lamb, J.J.; Burheim, O.S.; Pollet, B. Hydrogen fuel cells and water electrolysers. In *Micro-Optics and Energy: Sensors for Energy Devices*; Springer: Berlin/Heidelberg, Germany, 2020.
157. Yang, G.; Leitão, C.; Li, Y.; Pinto, J.; Jiang, X. Real-time temperature measurement with fiber Bragg sensors in lithium batteries for safety usage. *Measurement* **2013**, *46*, 3166–3172. [CrossRef]
158. David, N.A.; Wild, P.M.; Hu, J.; Djilali, N. In-fibre Bragg grating sensors for distributed temperature measurement in a polymer electrolyte membrane fuel cell. *J. Power Sources* **2009**, *192*, 376–380. [CrossRef]
159. Nascimento, M.; Novais, S.; Leitão, C.; Domingues, M.F.; Alberto, N.; Antunes, P.; Pinto, J.L. Lithium batteries temperature and strain fiber monitoring. In Proceedings of the 24th International Conference on Optical Fibre Sensors, Curitiba, Brazil, 28 September–2 October 2015; International Society for Optics and Photonics: Bellingham, WA, USA, 2015; Volume 9634, p. 96347V.
160. Sommer, L.W.; Raghavan, A.; Kiesel, P.; Saha, B.; Schwartz, J.; Lochbaum, A.; Ganguli, A.; Bae, C.-J.; Alamgir, M. Monitoring of intercalation stages in lithium-ion cells over charge-discharge cycles with fiber optic sensors. *J. Electrochem. Soc.* **2015**, *162*, A2664. [CrossRef]
161. Sommer, L.W.; Kiesel, P.; Ganguli, A.; Lochbaum, A.; Saha, B.; Schwartz, J.; Bae, C.-J.; Alamgir, M.; Raghavan, A. Fast and slow ion diffusion processes in lithium ion pouch cells during cycling observed with fiber optic strain sensors. *J. Power Sources* **2015**, *296*, 46–52. [CrossRef]
162. Bae, C.; Manandhar, A.; Kiesel, P.; Raghavan, A. Monitoring the strain evolution of lithium-ion battery electrodes using an optical fiber Bragg grating sensor. *Energy Technol.* **2016**, *4*, 851–855. [CrossRef]
163. Raghavan, A.; Kiesel, P.; Sommer, L.W.; Schwartz, J.; Lochbaum, A.; Hegyi, A.; Schuh, A.; Arakaki, K.; Saha, B.; Ganguli, A. Embedded fiber-optic sensing for accurate internal monitoring of cell state in advanced battery management systems part 1: Cell embedding method and performance. *J. Power Sources* **2017**, *341*, 466–473. [CrossRef]
164. Ganguli, A.; Saha, B.; Raghavan, A.; Kiesel, P.; Arakaki, K.; Schuh, A.; Schwartz, J.; Hegyi, A.; Sommer, L.W.; Lochbaum, A. Embedded fiber-optic sensing for accurate internal monitoring of cell state in advanced battery management systems part 2: Internal cell signals and utility for state estimation. *J. Power Sources* **2017**, *341*, 474–482. [CrossRef]
165. Song, Y.; Liu, D.; Liao, H.; Peng, Y. A hybrid statistical data-driven method for on-line joint state estimation of lithium-ion batteries. *Appl. Energy* **2020**, *261*, 114408. [CrossRef]
166. Feng, F.; Teng, S.; Liu, K.; Xie, J.; Xie, Y.; Liu, B.; Li, K. Co-estimation of lithium-ion battery state of charge and state of temperature based on a hybrid electrochemical-thermal-neural-network model. *J. Power Sources* **2020**, *455*, 227935. [CrossRef]
167. Hu, X.; Jiang, H.; Feng, F.; Liu, B. An enhanced multi-state estimation hierarchy for advanced lithium-ion battery management. *Appl. Energy* **2020**, *257*, 114019. [CrossRef]
168. Huang, C.; Wang, Z.; Zhao, Z.; Wang, L.; Lai, C.S.; Wang, D. Robustness evaluation of extended and unscented Kalman filter for battery state of charge estimation. *IEEE Access* **2018**, *6*, 27617–27628. [CrossRef]

169. Yang, S.; Deng, C.; Zhang, Y.; He, Y. State of charge estimation for lithium-ion battery with a temperature-compensated model. *Energies* **2017**, *10*, 1560. [CrossRef]
170. Zhang, Y.; Shang, Y.; Cui, N.; Zhang, C. Parameters identification and sensitive characteristics analysis for lithium-ion batteries of electric vehicles. *Energies* **2018**, *11*, 19. [CrossRef]
171. Shen, P.; Ouyang, M.; Lu, L.; Li, J.; Feng, X. The co-estimation of state of charge, state of health, and state of function for lithium-ion batteries in electric vehicles. *IEEE Trans. Veh. Technol.* **2017**, *67*, 92–103. [CrossRef]
172. Yu, Q.; Xiong, R.; Lin, C.; Shen, W.; Deng, J. Lithium-ion battery parameters and state-of-charge joint estimation based on H-infinity and unscented Kalman filters. *IEEE Trans. Veh. Technol.* **2017**, *66*, 8693–8701. [CrossRef]
173. Wang, Q.; Kang, J.; Tan, Z.; Luo, M. An online method to simultaneously identify the parameters and estimate states for lithium ion batteries. *Electrochim. Acta* **2018**, *289*, 376–388. [CrossRef]
174. CALCE Battery Research Group. CALCE Battery Group. Available online: https://web.calce.umd.edu/batteries/index.html# (accessed on 3 May 2021).